

Figure 7 Simulation (anisostructural model) of tensile and compressive at a constant strain rate of 1.2×10^{-3} /s with the original optimised data.

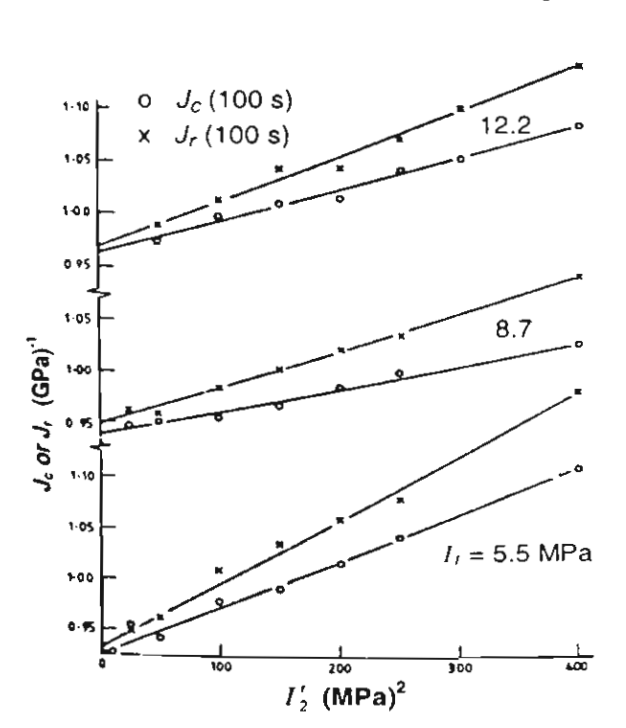


Figure 8 Plot showing the effect of I_2' on shear creep J_c (100s) and recovery J_r (100s) compliance at constant I_1 [Resen 1988] at 30° C.

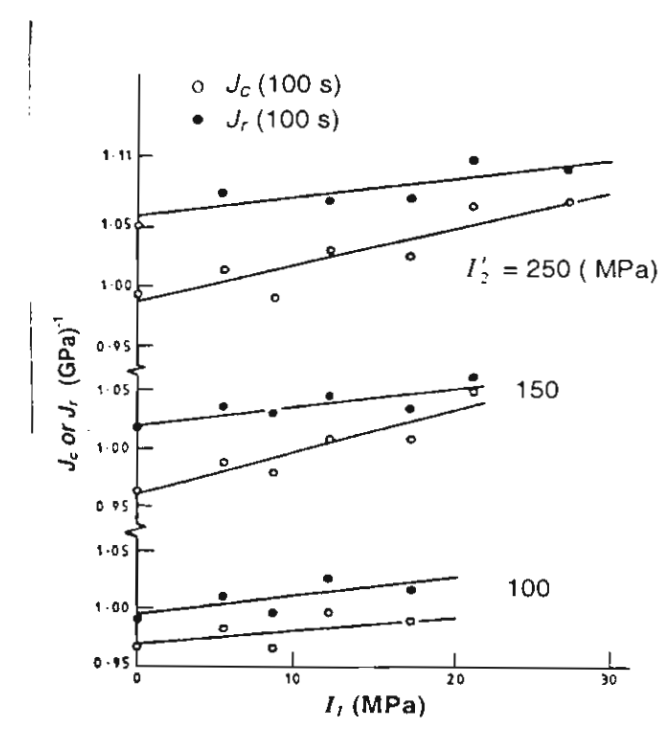


Figure 9 Plot showing the effect of I_I on shear creep J_c (100s) and recovery J_r (100s) compliance at constant I'_2 [Resen1988] at 30°C.

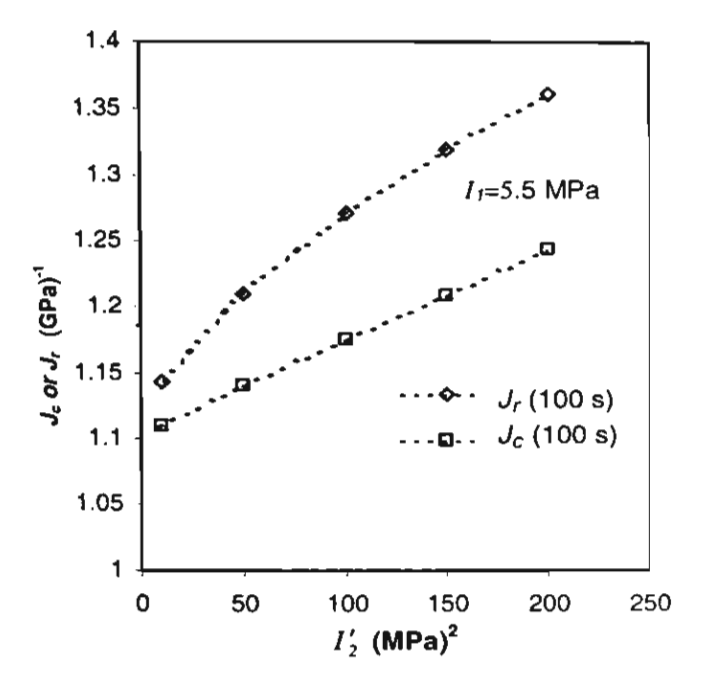


Figure 10 A comparison of creep J_c , and recovery J_r compliance at 100 sec under a constant I_I from simulated tension/torsion creep and recovery at 70°C.

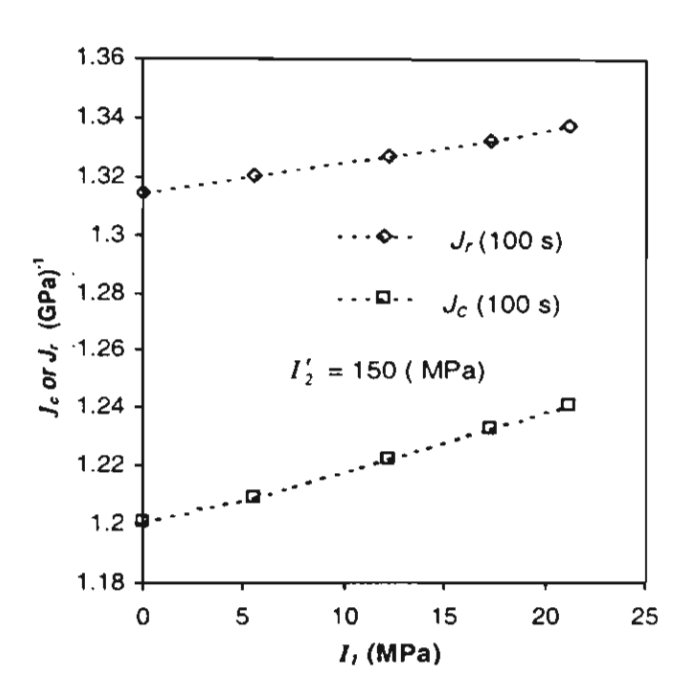


Figure 11 A comparison of creep, Jc, and recovery, Jr compliance at 100 sec under a constant I_2' from simulated tension/torsion creep and recovery at 70°C.

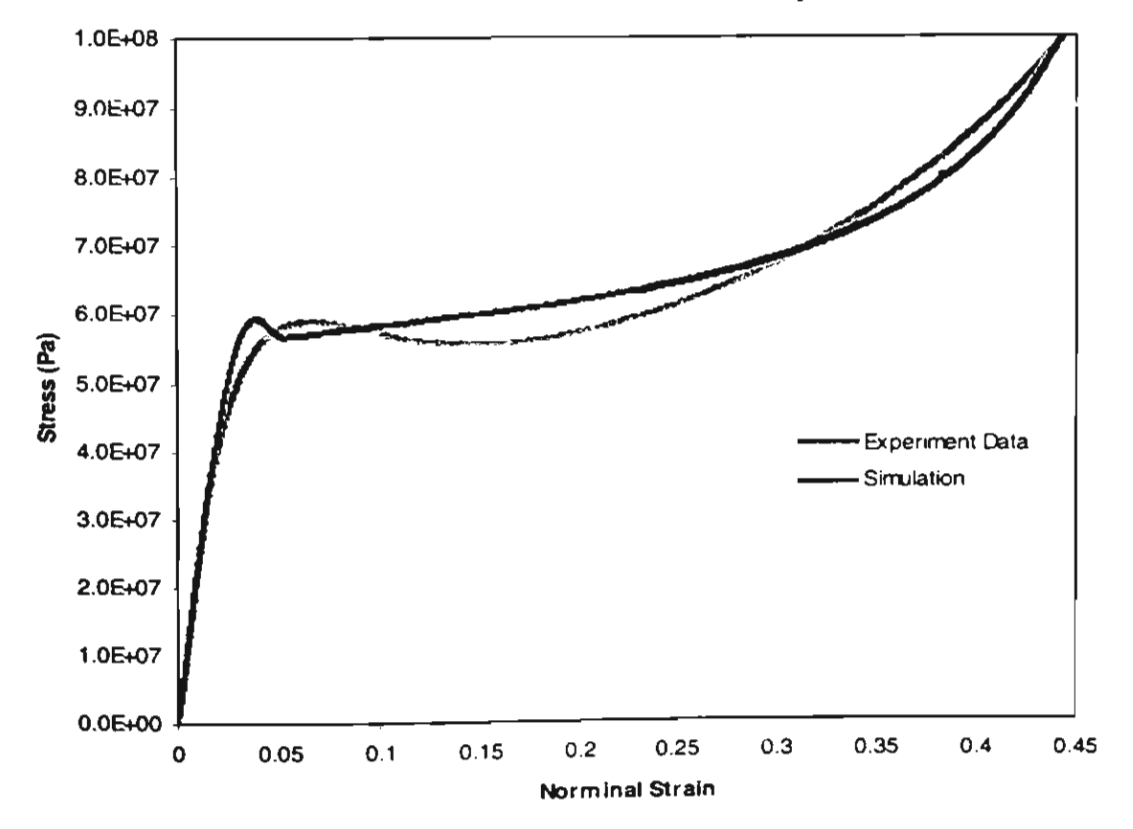


Figure 12 Comparison of numerical simulations (anisostructure constitutive model with strain hardening implemented) and compressive experimental data at strain rate = 1.2×10^{-4} /s.

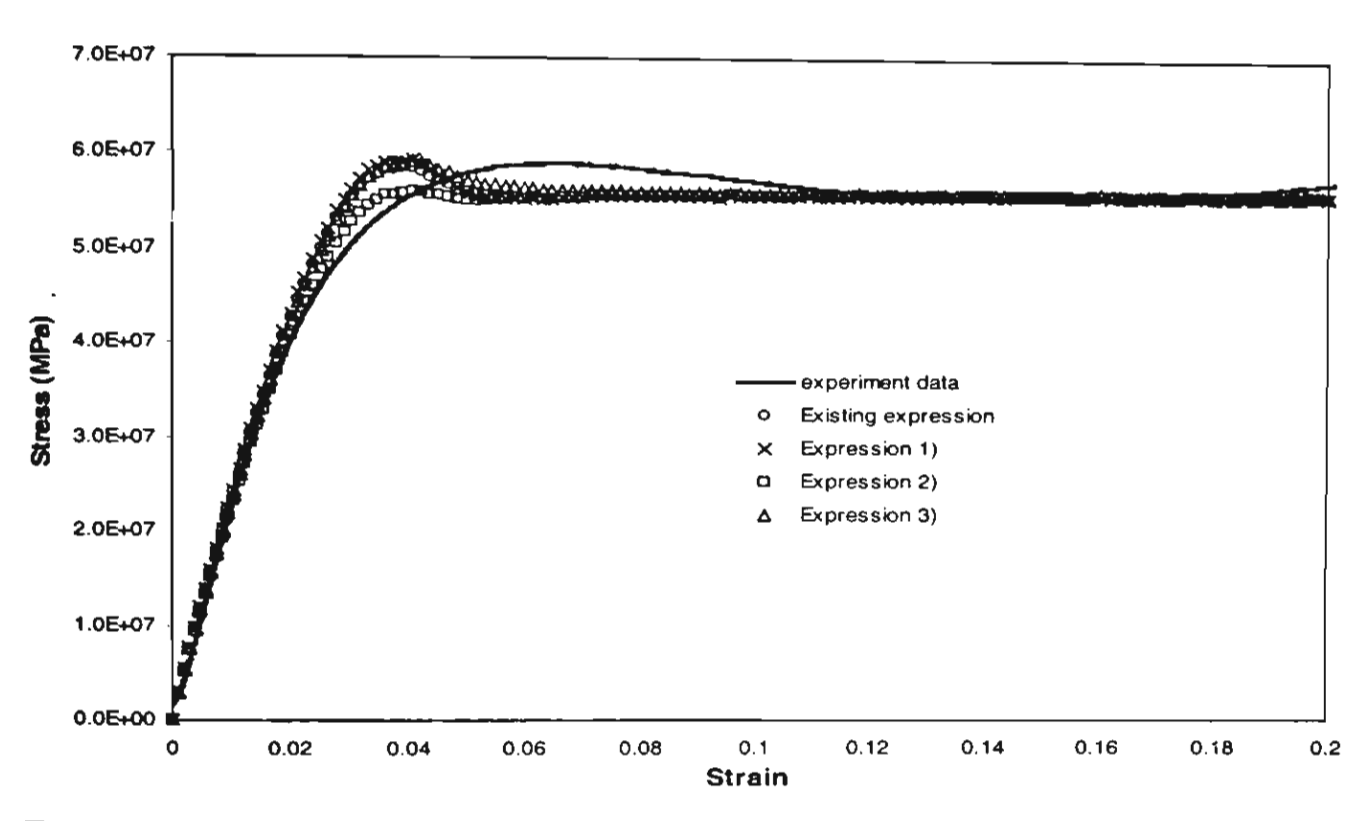


Figure 13 Simulation (anisostructural model) of compressive test at a constant strain rate of 1.2×10^{-4} /s. with various expression of T_f evolution described in Eqn 15. –Eqn 17.

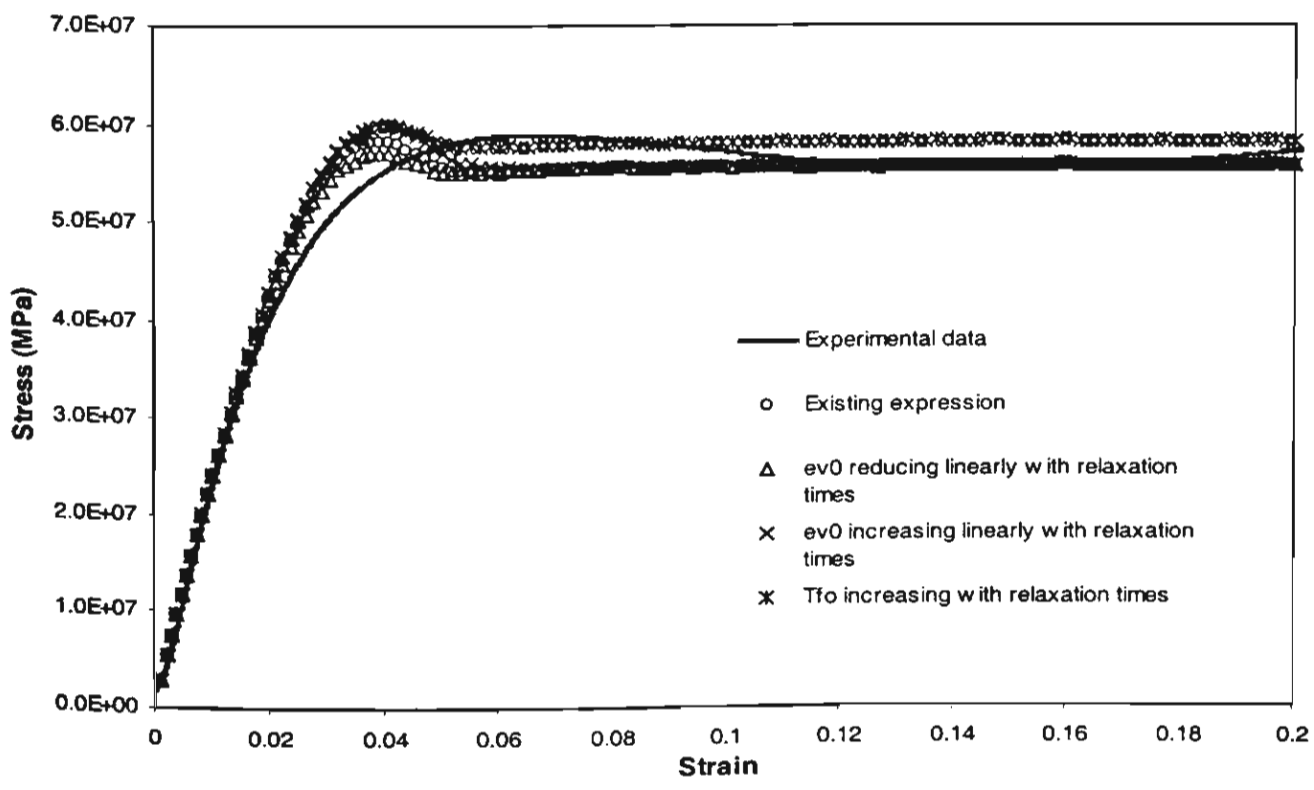


Figure 14 Simulation (anisostructural model) of compressive at a constant strain rate of 1.2 x 10^{-4} /s. with ϵ_0^{ν} and T_{fo} varying across the relaxation spectrum.

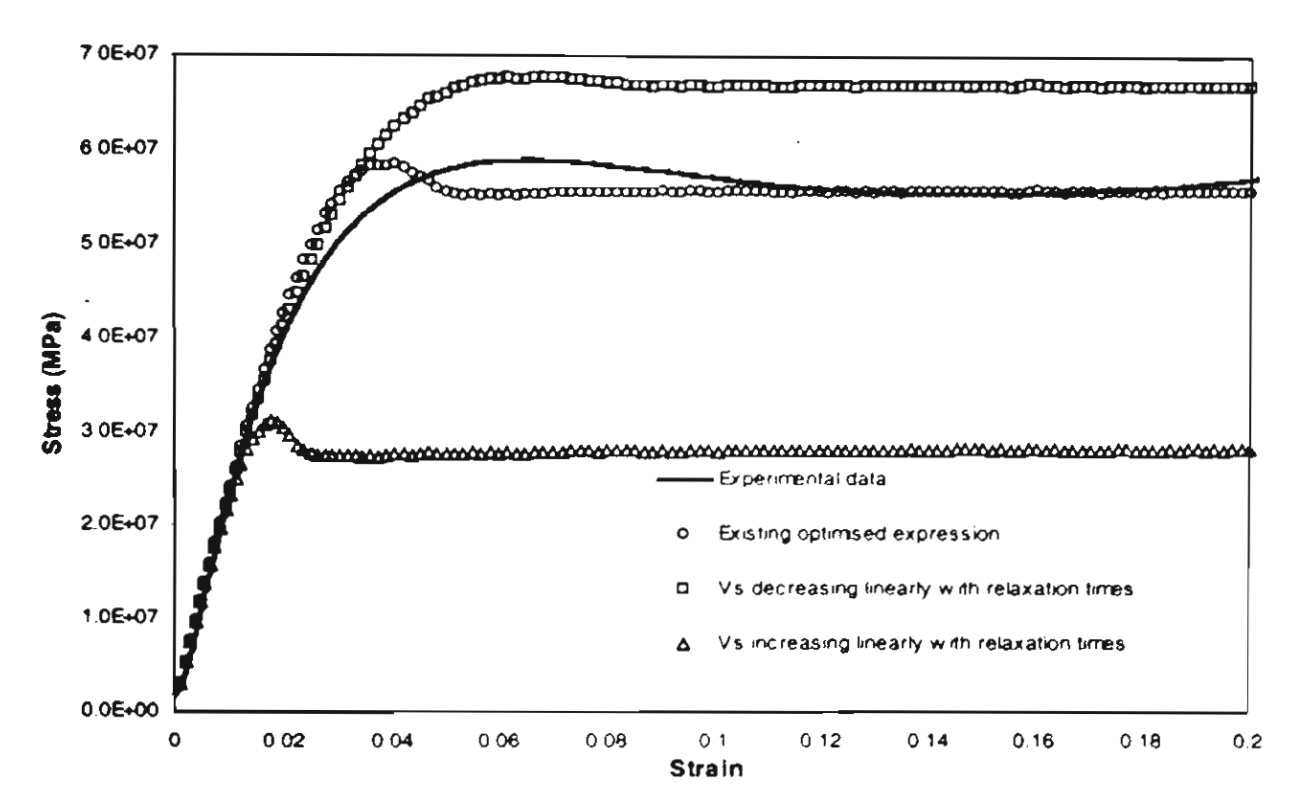


Figure 15 Simulation (anisostructural model) of compressive test at a constant strain rate of 1.2 x 10⁻⁴/s, with V, varying (linearly decreasing and increasing) across the relaxation spectrum

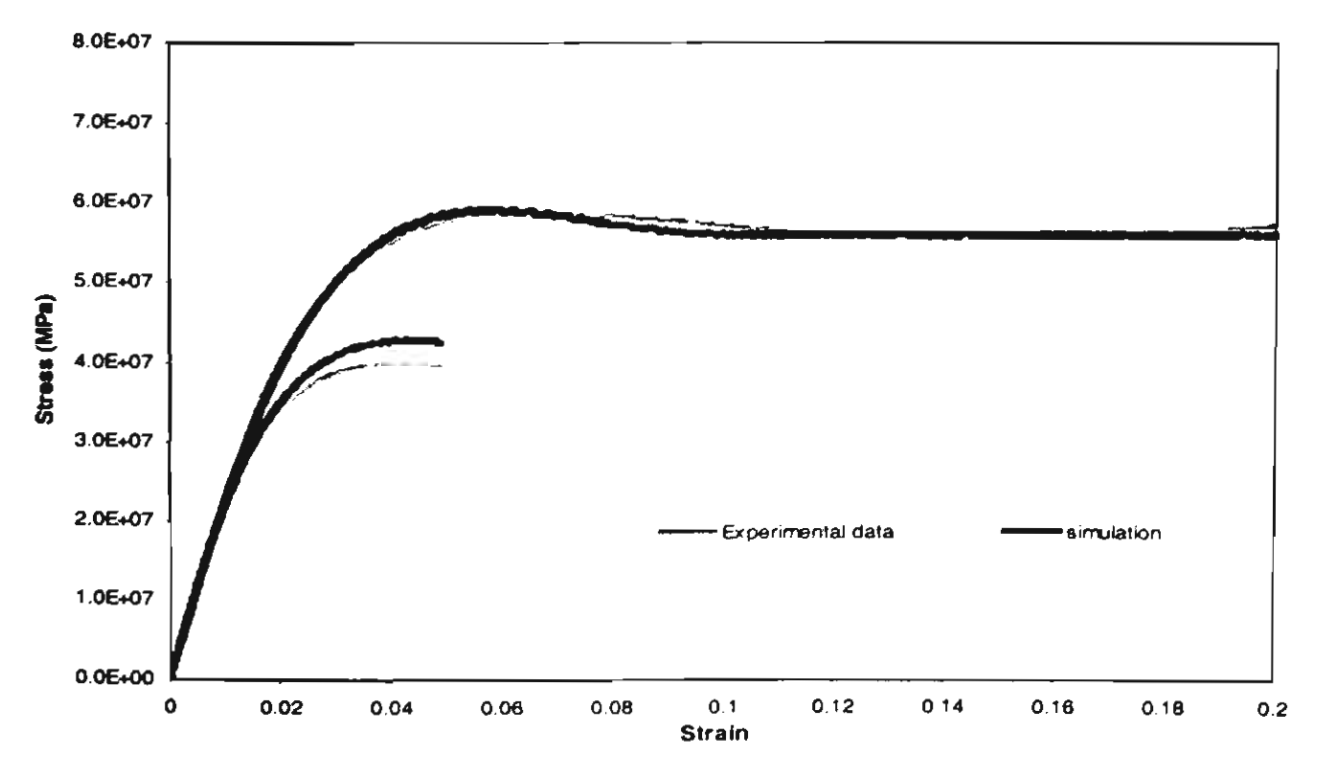


Figure 16 Simulation of tensile and compressive tests at a constant strain rate of 1.2×10^{-4} /s with new optimised parameters (V_3 decreasing linearly across the relaxation)

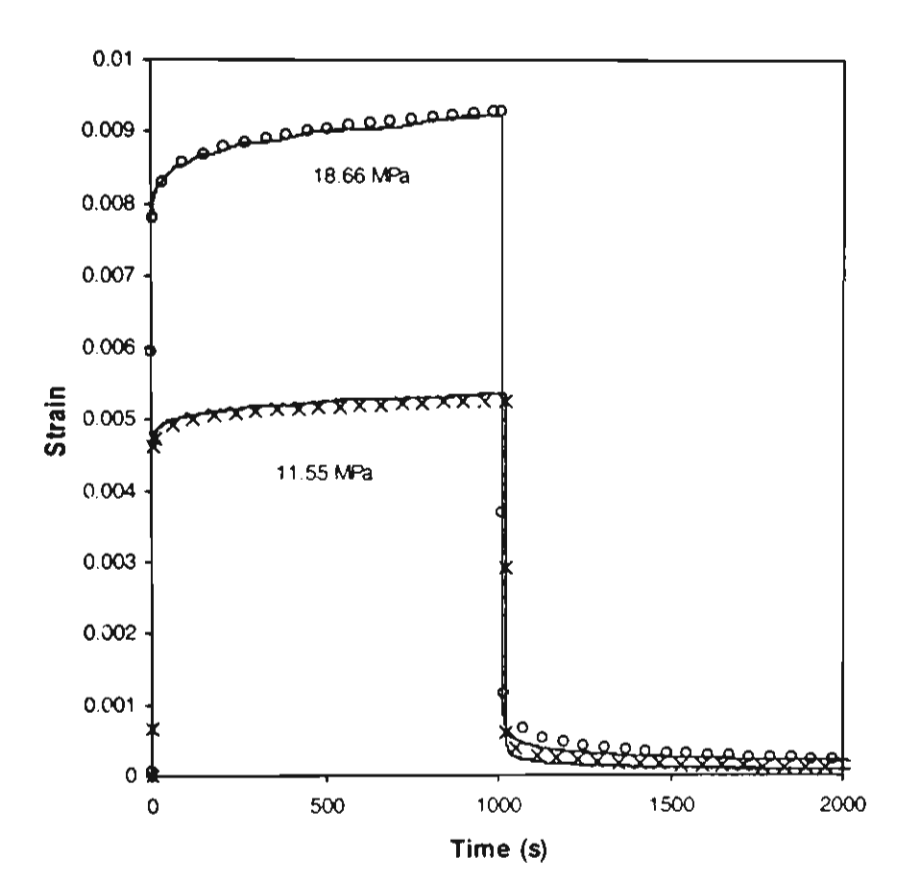


Figure 17 Simulation of a series of creep and recovery data using the *anisostructural* model for 1,000 seconds creep with new optimised parameters (Simulations are continuous line and data are symbols)

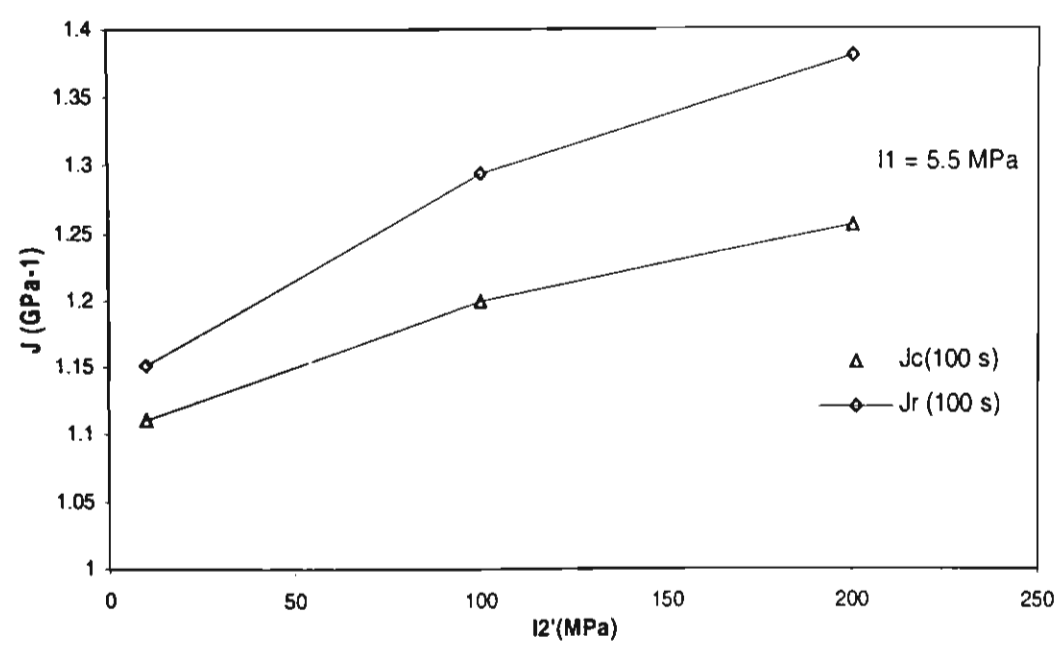


Figure 18 A comparison of creep compliance, J_c , and recovery compliance, J_r , at 100 sec under a constant I_I from simulated tension/torsion creep and recovery at 70°C with new optimised parameters.

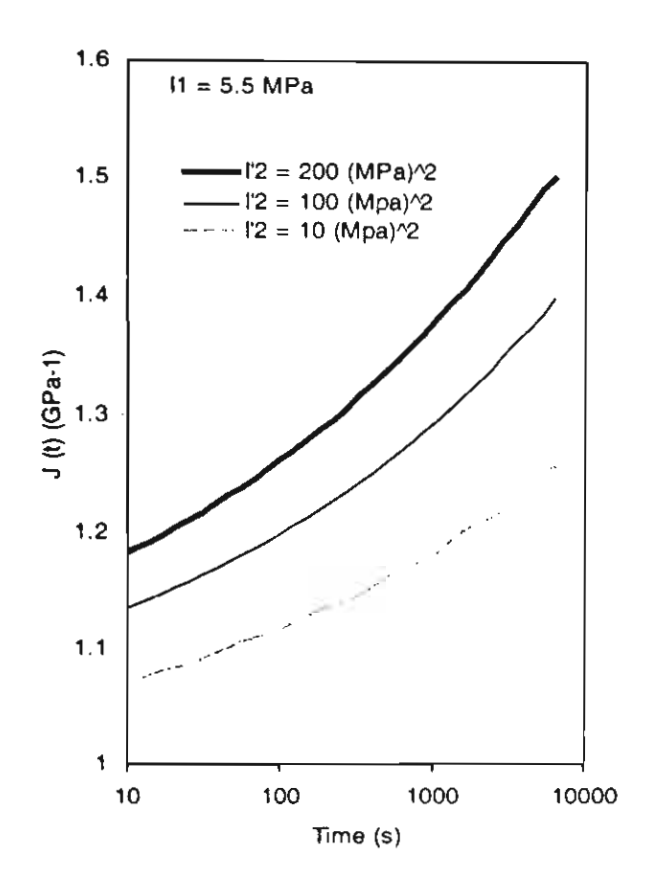


Figure 19 The simulation (anisostructural model) of time dependent creep compliance under a constant I1 with new optimised parameters.

Output จาก โครงการวิจัยที่ได้รับทุนจาก สกว.

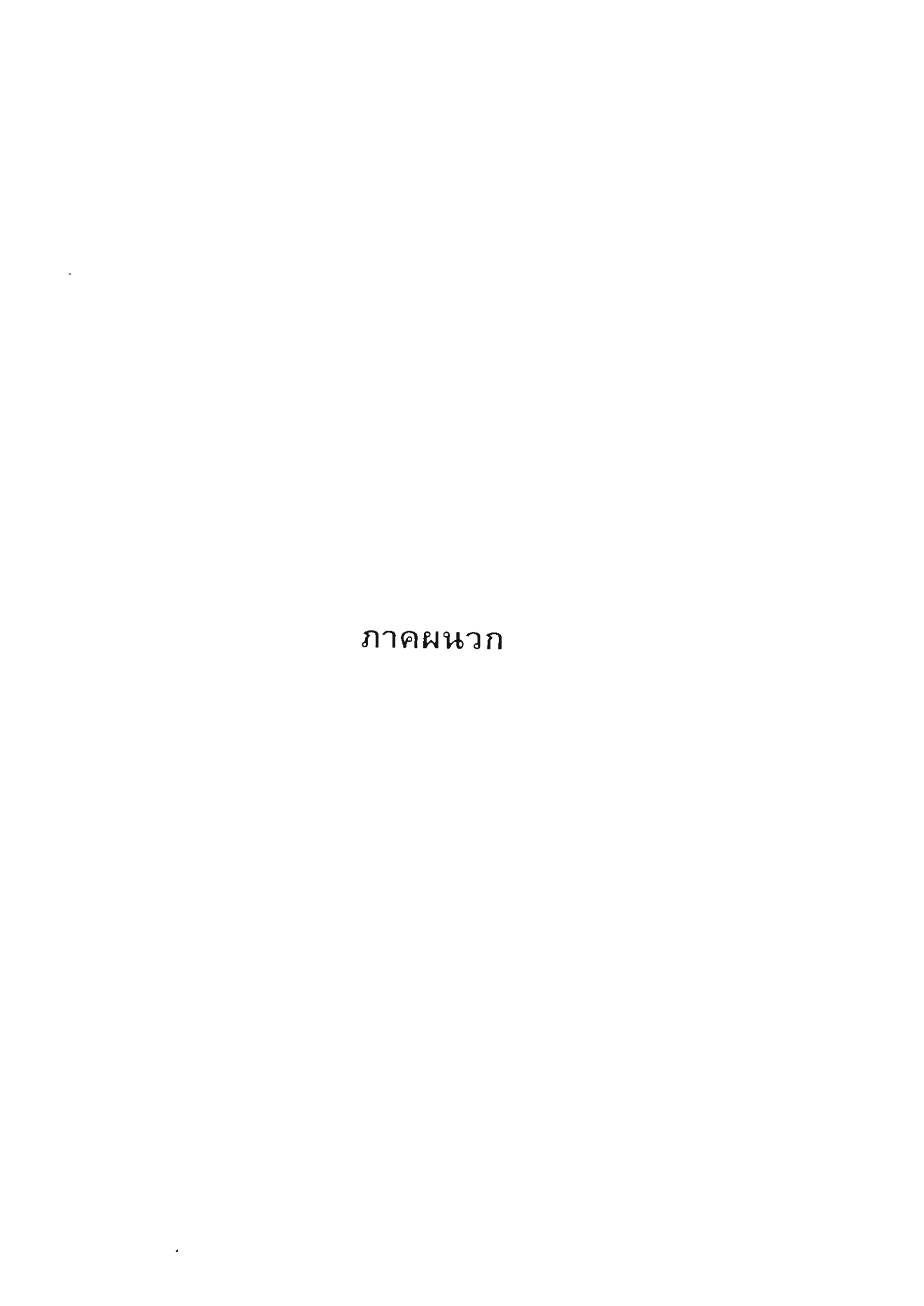
1. ผลงานการตีพิมพ์ในวารสารวิชาการนานาชาดิ:

อยู่ในระหว่างการเตรียมการเพื่อส่งบทความให้กับวารสารวิชาการนานาชาติ Mechnics of Time-Dependent Materials

2. การนำผลงานวิจัยไปใช้ประโยชน์:

ได้นำความรู้ที่ได้จากการวิจัยไปใช้ในการพัฒนาการเรียนการสอนวิชา Mechanics of Composite and Polymeric Materials ในหลักสูตรปริญญามหาบัณฑิต ภาควิชาวิศวกรรมเครื่องกล คณะวิศวกรรม ศาสตร์ สถาบันเทคโนโลยีพระจอมเกล้าพระนครเหนือ

3. อื่นๆ -



On the improvement of the anisostuctural constitutive model for describing deformation behaviour of glassy polymers

Arisara Chaikittiratana

Department of Mechanical Engineering, King Mongkut's Institute of Technology North Bangkok, 1518 Piboonsongkram Road, Bangkok 10220. Thailand; Email: acn@kmitnb.ac.th

C. Paul Buckley

Department of Engineering Science, University of Oxford, Parks Road, Oxford OX1 3PJ, UK

1. Abstract

The ultimate challenge in constitutive modelling of glassy polymers is to combine all the important aspects of deformation of polymer glasses in a single constitutive model and thus be able to describe the behaviour of a material in the widest range, and under the various modes of loading and boundary conditions.

A number of models have been developed recently, attempting to fulfil such need. However a single constitutive model which can show accurately, the nonlinear viscoelastic response under complex loading history, especially during unloading which polymers exhibit 'enhanced recorvery', yield drop and strain hardening behaviour, has never been reported before in the literature. The aim of the work is to extend the anisostructural model in the form developed earlier in the work of Chaikittiratana [2000] further such that it can describe more realistic yield behaviour and to include the feature of strain hardening after yield

2. Introduction

Accurate stress-strain analysis of glassy engineering polymers becomes increasingly important as these polymers are expected to perform as reliably and predictably in various loading

applications. However these materials pose a particular challenge, in view of the rich variety of nonlinear viscoelastic features seen in their constitutive responses. To achieve trustworthy stress-strain analysis, a nonlinear viscoelastic constitutive model capable of faithfully describing the response to time-dependent, multiaxial stress histories is required.

Polymers are viscoelastic materials displaying time dependent but recoverable deformation. Unlike metals, significant viscoelastic behaviour of polymers, such as creep and stress relaxation can be observed at all temperatures and is dependent on the history of stress, strain, and temperature in a very complex manner.

In load-bearing applications polymer parts are often subjected to multiaxial and complex stress histories, including loading and unloading, and the deformations are usually in non-linear viscoelastic regime. However, non-linear viscoelastic stress-strain analysis for polymers, requires accurate constitutive modelling to describe precisely the response to time-dependent, multiaxial stress histories. To date, the subject of the modelling of nonlinear viscoelastic behaviour remains a very active field of research.

A number of constitutive models have been developed to describe the nonlinear viscoelastic behaviour of polymers. Most of the constitutive models have been aimed at different aspects of the observations, such as the yield phenomenon, creep, stress relaxation, rate dependency during monotonic loading, strain softening and strain hardening. Frequently one model deals with only one aspect of the behaviour and other aspects are not considered. Few models attempted to predict the nonlinear viscoelastic behaviour of various deformation modes.

In the work of Chaikittiratana [2000], a new improved mathematical constitutive model was proposed. The new model was based on the existing 3-D isostructural constitutive model by Dooling et al [1998] which assumed that the physical state of the glass structure are not changed

during deformation and the non-linearity simply arises from the effect of the local stress raising the local free energy. The *isostructural* model can describe tension—torsion creep but can not capture recovery after unload and strain softening. In the improved model, the *isostructural* assumption was opted out and replaced with the *anisostructural* assumption which assumed that the physical state of glassy structure as notified by a fictive temperature T_f varies with the effective viscous strain in a manner which T_f is initially increasing with the effective viscous strain and then reaches a saturation. By assuming that each relaxation time has its own fictive temperature changing with the local effective viscous strain in the environment of that relaxation time, it was found that the improved model could capture correctly the feature of the 'enhanced recovery' commonly observed in glassy polymers and displayed feature of strain softening.

The work presented here describes how the anisostructural model developed in the work of Chaikittiratana [2000] can be improved further such that the feature of strain hardening after yield and realistic yield behaviour can be captured.

3. The anisostructural model

The basis of the anisostructural model developed in the work of Chaikittiratana [2000] is the model proposed for isotropic glassy polymers below the glass transition by Dooling, Buckley and Hinduja[1998] (DBH), itself a small-strain spectral generalization of the Glass-Rubber model of Buckley and Jones[1995]. According to DBH, the macroscopic stress σ is obtained from a set of N+1 tensor state variables

$$\boldsymbol{\sigma} = \sum_{j=1}^{N} v_j \boldsymbol{\sigma}_j^{b} + \boldsymbol{\sigma}^{c} \tag{1}$$

representing contributions from primary and secondary bond-stretching in N different environments within the glass (σ_j^b) and from conformational entropy change (σ_j^c) . Each weighting factor v_j (which may be considered the volume fraction associated with environment j) is associated instantaneously with a shear relaxation time τ_j . Stress and deformation are separated into deviatoric (nonlinear viscoelastic) and hydrostatic (linear elastic) parts, with the deviatoric component of σ_j^b evolving according to

$$\dot{\mathbf{s}}_{j}^{b} + \frac{\mathbf{s}_{j}^{b}}{\tau_{i}} = 2G^{b}\mathbf{e} \tag{2}$$

where s and e are deviatoric stress and strain respectively. G^b is the corresponding shear modulus. Nonlinearity enters the original (isostructural) DBH model through stress-dependence of the relaxation times, expected from the nonlinear dependence of transition rates on activation barrier height. However, in view of the evidence for strain-induced structural rejuvenation, we now generalize the model to the anisostructural case. For consistency with the extensive literature on structural evolution in glasses, we represent the glass structure at any instant by Tool's fictive temperature T_f – temperature at which it would possess the same relaxation time at equilibrium. The j-th relaxation time is now related to its value $\tau_{0,j}$ in the linear viscoelastic limit, through shift factors $a_{\sigma,j}$ and $a_{\tau_{t,j}}$ respectively

$$\tau_{j} = a_{\sigma,j} a_{T_{f,j}} \tau_{0,j}, \quad a_{\sigma,j} = \frac{V_{s} s_{\text{oct},j}^{b}}{2RT} \frac{\exp\left(\frac{-V_{p} \sigma_{m}^{b}}{RT}\right)}{\sinh\left(\frac{V_{s} s_{\text{oct},j}^{b}}{2RT}\right)}, \quad a_{T_{f,j}} = \exp\left(\frac{C}{T_{f,j} - T_{\infty}} - \frac{C}{T_{f0} - T_{\infty}}\right)$$
(3)

where $\sigma_{\rm m}^{\rm b}$, $s_{{\rm oct},j}^{\rm b}$ are mean stress and j-th octahedral shear stress respectively, $V_{\rm s}$, $V_{\rm p}$, C and $T_{\rm oc}$ are material constants and $T_{\rm f0}$ is the initial fictive temperature. Evidence from post-yield strain-softening shows that structural rejuvenation saturates. A simple two-parameter function with this feature was used therefore to describe the dependence of $T_{\rm f,j}$ on deviatoric viscous strain:

$$T_{f,j} = T_{f0} + (T_{f\infty} - T_{f0}) \left[1 - \exp\left(-\frac{\overline{\varepsilon}_{j}^{v}}{\varepsilon_{0}^{v}} \right) \right] \quad \text{where} \quad \overline{\varepsilon}_{j}^{v} = \sqrt{\frac{2}{3} \left(\varepsilon_{j}^{v} : \varepsilon_{j}^{v} \right)}$$
 (4)

where $T_{f\infty}$ is the (material-specific) saturation fictive temperature and $\varepsilon_0^{\mathsf{v}}$ is another material constant, and $\varepsilon_j^{\mathsf{v}}$ is the tensor of j-th viscous strain. The reader should note that, in the new spectral version of the model, the local (j-th) viscous strain determines $a_{\tau_i,j}$. This was found to be a necessary condition for correct replication of the recovery anomaly. A notable feature of the model is its small number of adjustable parameters. For a polymer with given initial structure T_{f0} , there are just four adjustable parameters to capture the entire range of deviations from linear viscoelasticity ($V_s, V_0, T_{f\infty}, \varepsilon_0^{\mathsf{v}}$).

The new constitutive model was applied to well-aged, isotropic cast poly(methyl methacrylate) (PMMA) at 70°C. The material response was fully characterized using a programme of tensile creep and stress relaxation tests, and constant extension-rate tension and compression tests, all executed with a standard Instron 4204 testing machine and Instron 3119 Series environmental chamber. Specimen deformation was measured using Instron extensometers: model 2620-603 for creep and stress relaxation experiments and model 2620-604 for constant extension-rate tests. A discrete shear relaxation spectrum was fitted to long-term linear viscoelastic creep data, and then the nonlinearity parameters were fitted to other data by an iterative manual routine. The

"universal" value of 1.3 [Bauwens-Crowet 1973] was assumed for the ratio of compression to tension yield stress, and $T_{\rm f0}$ was taken to be 378K.

Illustrations of the fit between model response and creep and recovery experiments well into the non-linear viscoelastic region are shown in Figure 1, for different creep stresses. The model also correctly describes post-yield strain-softening in compression, as can be seen in Figure 2. However it under-predicts the yield strain, and experimental data in compression show more gradual yield than the model. It may be seen that the model over-predicts the apparent yield stress in tension – this is likely to be an artifact caused by crazing intervening in the experimental data.

The stress-state dependence of the model was tested by simulating a program of biaxial (tension+shear) non-linear viscoelastic creep and recovery experiments, exploring dependence on the stress invariants $I_1 = tr\sigma$ and $I'_2 = \frac{1}{2}s : s$. The predicted recovery anomaly was found to increase with I'_2 but not with I_1 , in accord with experiment for PMMA [Resen 1988]. Figure 3 illustrates this for the predicted 100 s shear creep compliance as obtained from simulations of creep and recovery, $J_c(100 \text{ s})$ and $J_r(100 \text{ s})$ respectively, for constant I_1 and varying I'_2 .

4. Implementation of strain hardardening behaviour

The strain-hardening behavior in glassy polymers is generally attributed to rubber-like entropic elasticity, arising from the reducing entropy of aligning mobile chains. The strain hardening behaviour is implemented in to the current form of the anisostructure model for PMMA. In the present work, we follow usual practice to invoke a conformational entropy function when calculating this part of the stress. The deviatoric component conformational stress S_i^c can be

obtained directly from differentiation of the conformational free energy density A^c which is described in terms of the deviatoric principal network stretches $\overline{\lambda}_i$ (i=1..3). There are many suggestions have been made for A^c . In this work we employed the energy function used is that derived by Edwards and Vilgis [1986]. Thus, now the conformational contribution to the principal components of deviatoric stress S_i^c can be expressed as:

$$S_i^c = \overline{\lambda}_i \frac{\partial A^c}{\partial \overline{\lambda}_i}$$
 (i =1..3)

where;

$$A^{c} = \frac{N_{s}k_{b}T}{2} \left[\frac{(1+\eta)(1-\alpha^{2})}{1-\alpha^{2}\sum_{i=1}^{3}\overline{\lambda}_{i}^{2}} \sum_{i=1}^{3}\overline{\lambda}_{i}^{2} + \sum_{i=1}^{3}\ln(1+\eta\overline{\lambda}_{i}^{2}) + \ln\left(1-\alpha^{2}\sum_{i=1}^{3}\overline{\lambda}_{i}^{2}\right) \right]$$
(6)

 N_s is the number density of slip-links (entanglements), η is parameter specifying the looseness of the entanglements, and α is a measure of the inextensibility of the entanglement network. The Cauchy stress tensor can be fully defined by

$$\mathbf{\sigma} = \mathbf{S}^b + \mathbf{S}^c + \sigma_m \mathbf{I} \quad ; \quad \sigma_m = K\phi \tag{7}$$

K is bulk modulus and ϕ is dilation. Under the assumption of no chemical cross-links, the corresponding parameters are the slip-link (entanglement) density N_s , the inextensibility factor α , and the slip-link mobility factor η . It was found that the best fit can be obtained with $\eta = 0.0$, $\alpha = 0.47$ and $N_s = 3.0 \times 10^{26}$. Figure 4 shows the model simulation together with the experimental data. Although a perfect fit can not be obtained, a uniaxial compressive strain hardening behaviour can be captured by the model moderately well. However, slight increase in the magnitude of stress drop can be observed due to the strain hardening effect.

5. Yield peak broadening

Although the new anisostructural constitutive model with local T_f assumption could give a good description of 1000 s creep and recovery in the non-linear viscoelastic regime, but the model predicted smaller strain at yield and a more abrupt yield peak than the experimental data. This suggests that some description in the constitutive model relating to yielding behaviour needs improvement.

By observing a plot of stress and strain of deformation under constant strain rate, initially the plot shows straight line reflecting linear elastic-like response. Then the slope of the plot begins to decrease gradually but sufficiently noticeable at a stress level approximated to half of the yield peak. This suggests that at this stress level, some portions in the material have already accessed to flowing process by some extent. In the constitutive model, the parameters which govern stress dependent of the viscoelasticity are the activation volumes V_s and V_p . The broad yield peak suggests that the stress dependent in flowing behaviour is different for different relaxing elements in the material. Thus it implies that the activation volumes are in fact varies across the discrete relaxation spectrum. It can be imagined that there are many possible molecular motions in the polymer system that can be activated each with its own activation parameters. As the temperature or strain rate varies, one or another of these mechanism may be dominant over the others.

The possibility of the variation of activation across the relaxation spectrum which was neglected previously in the model was re-included. In the work of Dooling and Buckley et al. [1998] the variation of the activation volume was assumed to varied linearly with the relaxation spectrum in the same manner of that ΔS and ΔH . The variation was assumed such that the longer relaxation times posses larger activation volumes, thus the parameter β was chosen as a possible

number. It is to be noted that β is only applied to V_3 . However, when apply positive number of β into the newly developed model, it did not improve the model's ability to capture gradual yielding, but a small negative values can. This is to be noted also that in the work of Dooling and Buckley et al.[1998], the relaxation spectrum used in that work is cut off at 10^7 , thus it unavoidably creates unrealistic non-linear deformation at high stresses and long time. This forced them to opt for the larger activation volumes for long relaxation times in order to reproduce the experimental data reported in their work. The negative values of β means that at smaller relaxation times, the quickest to be activated portions in material, have larger activation volumes indicating that they require smaller stress than the other portions to make sufficient rate of flow comparable to that of the imposed strain rate. Those who have large relaxation times will have smaller activation volumes, but they are those who carry most of the applied stress. Thus, in those portions, the flow process can occur with comparable rate with smaller activation volumes. By looking at the definition of the shear activation volume following Eyring et. Al.[1945] in Buckley and Jones [1995]

$$V_{s} = \frac{3V}{2} \Delta \gamma_{oct} \tag{8}$$

The activation event is taken to be a discrete viscous deformation of volume V of material obeying equation (viscous equation), the work ΔW done by the stress system modifying the energy barrier can be expressed in terms of the shear stress and increment of viscous shear strain as $\Delta W = V_s \tau_{oct}^b$. From this definition, there is a possibility that in the longer relaxation times elements, smaller shear strain can take place due to close packing around those portions, although the volume V of material involving the activation process could be larger. Thus it is possible that V_s are smaller for larger relaxation times.

By manual iteration following the similar process described previously, the initial best fit of the model to the constant strain rate experiment data was achieved by having the parameters as follows; $V_s^* = 0.0033 \text{ m}^3/\text{mol}$, $V_p^* = 0.00033 \text{ m}^3/\text{mol}$, β =-0.005, T_{f0} = 377.5 K, T_{f0} = 384 K and $\varepsilon_0^{\ \nu}$ = 0.00364. The comparison of the simulation and the constant strain rate experimental data is shown in Figure 5.

It can be seen from Figure 5 that now the anisostructure model with variation of shear activation volumes can correctly describe a yield stress, yield drop in compression and also capable of reproducing the feature of gradual yield. The model over-predicts the apparent yield stress in tension. However this is likely to be an artefact of crazing intervening in the experimental case as mentioned before.

The simulations of a series of creep and recovery experiments well into the non-linear viscoelastic region are shown together with the experiment data in Figure 6, for different creep stresses. It can be seen from the figure that the model can still capture very well the deformation behaviour of creep and recovery.

6. Conclusion

The features of creep-recovery, stress relaxation and yield drop in a glassy polymer can be captured with a anisostructural variant of the DBH model, where the fictive temperature varies with local viscous strain. The simulation of creep and recovery under different stress states, shows the same trends as that observed experimentally by Resen[1988].

However, the simulation of constant strain rate history predicts earlier yield and gives unrealistic abrupt yield peak. It was discovered that the broader yield peak, and hence more realistic yield behaviour, can be brought about by letting the shear activation volumes to vary

linearly across the discrete relaxation spectrum such that shorter relaxation times are associated with larger shear activation volumes. Furthermore, with this variation of shear activation volumes, the features of creep-recovery, especially the 'enhanced recovery', effects are still in accord with the experimental data performed by the author [2000]. Although the simulations of creep and recovery experiments are slightly poorer than with the constant activation volumes, this deficiency can certainly be improved by finer adjustment of the non-linear parameters.

The strain hardening feature was successfully implemented in to the existing anisostructural model employing Edwards-Vilgis strain energy function.

The constitutive model can now capture, the non-linear viscoelastic response under complex loading history, including unloading which polymers exhibit 'enhanced recorvery', yield drop and strain hardening behaviour. These features has never been reported before for a unified constitutive model in the literature.

7. Reference

Bauwens-Crowet, C. [1973]. Journal of materials science 8: 968.

Buckey, C.P. and D.C. Jones [1995]. Polymer 36: 3301.

Chaikittiratana, A. [2000]. Non-linear Viscoelastic Strain Analysis. D.Phil. Thesis.

Department of Engineering Science. University of Oxford. Oxford.

Dooling, P.J. and C.P. Buckley [1998]. Polymer Engineering and Science. 38:892.

Edwards, S. F. and T.H. Vilgis [1986]. Polymer, 27: 483

Halsey, G., H.J. White and H. Eyring [1945]. Textile Research Journal 15: 295.

Resen, A. S. [1988]. Biaxial creep of plastics. Ph.D., Department of Mechanical Engineering. Manchester, UMIST.

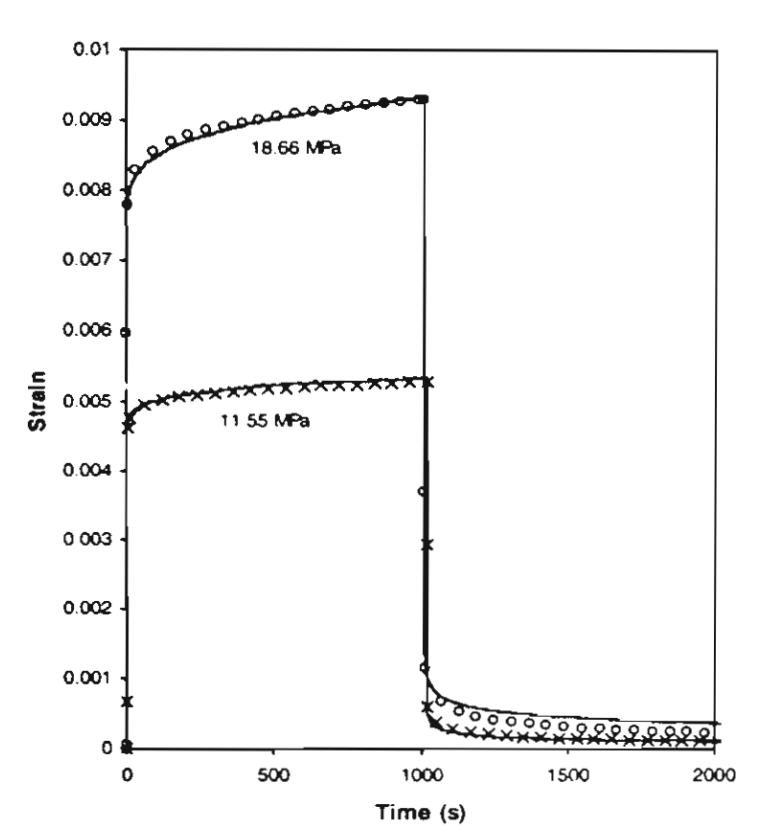
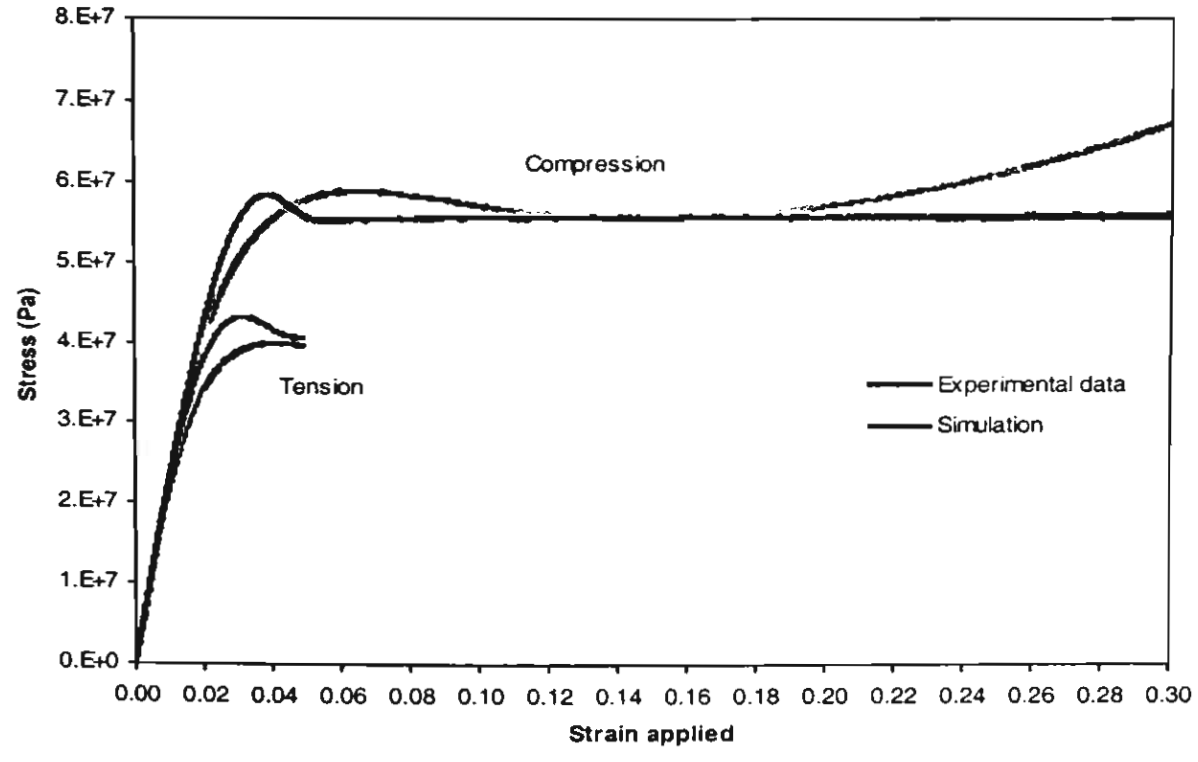


Figure 1 Simulation of a series of creep and recovery data using the new anisostructural model for 1,000 seconds creep.



gure 2 Simulation (anisostructural model) of tensile and compressive at a constant strain rate of 1.2 x 10⁻⁴/s.

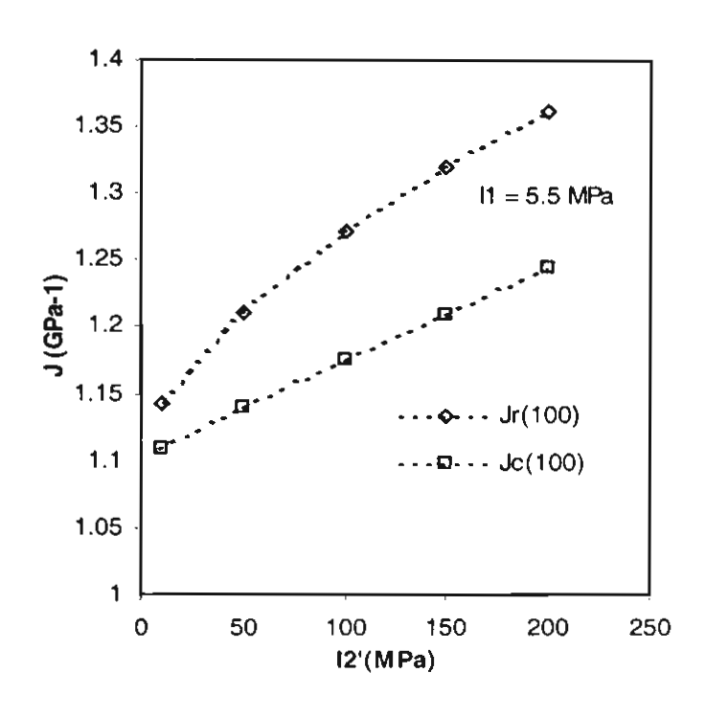


Figure 3 A plot of creep compliance, J_c , and recovery compliance, J_r , at 100 sec under a constant I_1 (I'_2 varying) from simulation at 70°C.

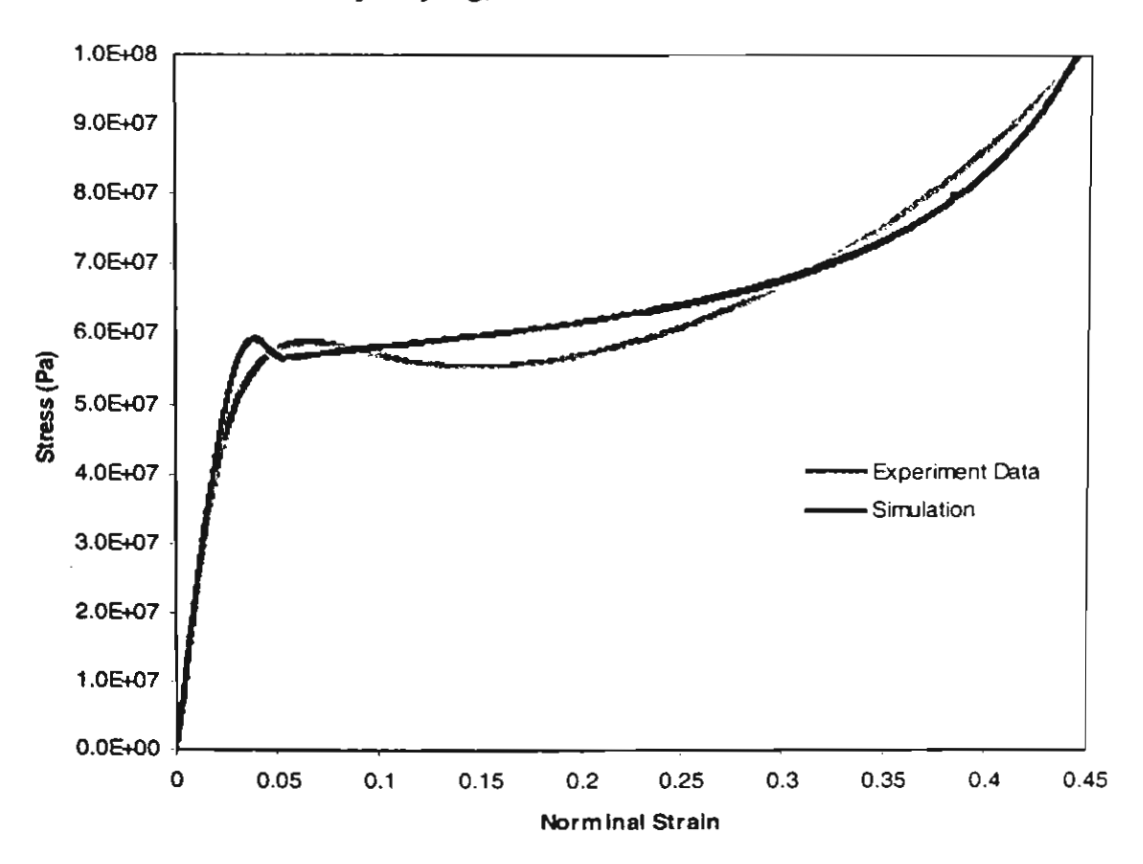


Figure 4 Comparison of numerical simulations (anisostructure constitutive model with strain hardening implemented) and compressive experimental data at strain rate = 1.2×10^{-4} /s.

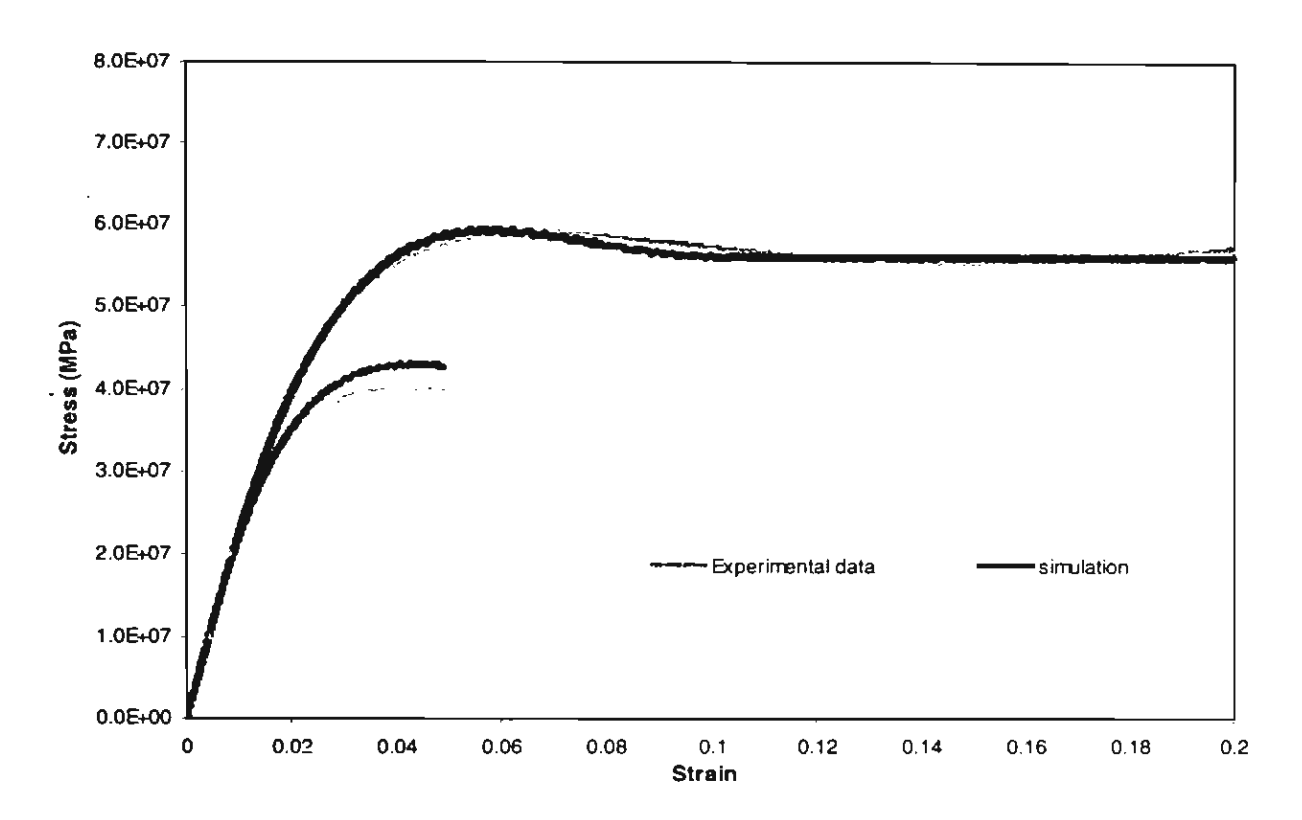


Figure 5 Simulation of tensile and compressive tests at a constant strain rate of 1.2×10^{-4} /s with new optimised parameters (V_s decreasing linearly across the relaxation)

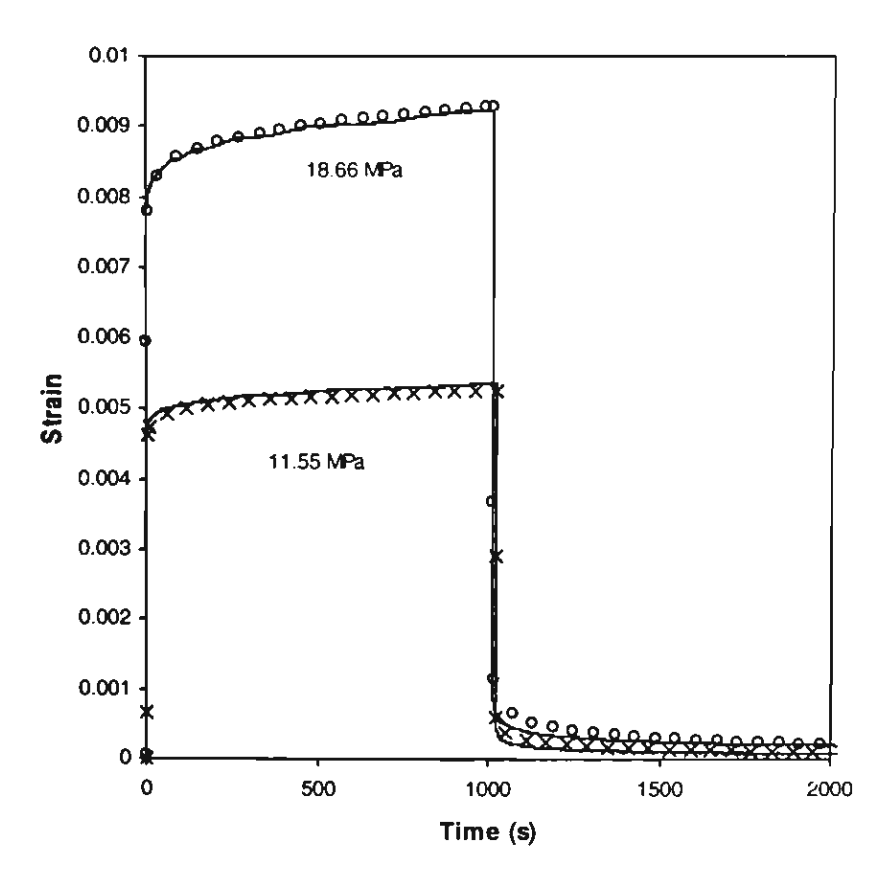


Figure 6 Simulation of a series of creep and recovery data using the *anisostructural* model for 1,000 seconds creep with new optimised parameters (Simulations are continuous line and data are symbols)